Article

A Doxorubicin-Loaded Photosensitizer-Core pH-Responsive Copolymer Nanocarrier for Combining Photodynamic Therapy and Chemotherapy

Xiaohan Zhang, Qiu Li, Xiaodong Sun, Baolei Zhang, Hongxiang Kang, Fuli Zhang, and Yiguang Jin

ACS Biomater. Sci. Eng., **Just Accepted Manuscript** • DOI: 10.1021/acsbiomaterials.6b00762 • Publication Date (Web): 15 Feb 2017

A Doxorubicin-Loaded Photosensitizer-Core pH-Responsive Copolymer Nanocarrier for Combining Photodynamic Therapy and Chemotherapy

Xiaohan Zhang,[†,‡] Qiu Li,[†,¶] Xiaodong Sun,[†,‡] Baolei Zhang,[†,‡] Hongxiang Kang,[†] Fuli Zhang,[‡] and Yiguang Jin[*,†,‡]

[†]Department of Pharmaceutical Sciences, Beijing Institute of Radiation Medicine, 27 Taiping Road, Beijing 100850, China, e-mail address: jinyg@sina.com

[‡]Institute of Pharmacy, Pharmaceutical College of Henan University, Kaifeng 475004, China

[¶]State Key Laboratory of Quality Research in Chinese Medicine, Institute of Chinese Medical Sciences, University of Macau, Avenida Padre Tomas Pereira, Taipa, Macao SAR, China

ABSTRACT: Photodynamic therapy (PDT) is an emerging method for the treatment of cancer. The combination of PDT and chemotherapy is a hot topic though the two therapies could not simultaneously exert their perfect effect *in vivo*. Here we report a doxorubicin-loaded photosensitizer-core pH-responsive copolymer nanocarrier with high tumor targeting and anticancer effects due to integration of PDT with chemotherapy. The pH-responsive photosensitizer-core four-armed star-shaped copolymer, [methoxy-poly(ethylene glycol)-poly(2-(N,N-diethylamino)ethyl methacrylate)-poly(ε-caprolactone)]$_4$-zinc β-tetra-(4-carboxyl benzyloxyl)phthalocyanine (PDCZP), was prepared, which was a molecular spherical nanocarrier in aqueous media. The carriers changed from small at high pH to large at low pH (51, 105, and 342 nm at pH 7.4, 6.5, and 5.0, respectively) and the zeta potential gradually increased (7.15, 16.2, and 26.1 mV at the above pH, respectively). PDCZP had a longer emission wavelength (max. 677 nm) than the parent photosensitizer, favoring light penetration through biological tissues. The singlet oxygen ($^1O_2$) quantum yield of PDCZP was 0.41. Doxorubicin (DOX) showed rapid release from PDCZP in the acidic media. More importantly, the drug-loaded nanocarrier showed the better *in vitro* and *in vivo* anticancer effects under lighting on MCF-7, SW480 cells and HepG2 cells and the murine hepatocellular carcinoma H_{22} models than the other groups. PDCZP showed a high tumor targeting effect based on the enhanced permeation and retention effect and its small size. The photosensitizer-core nanocarrier is a promising photodynamic nanocarrier for integrating other therapies.

KEYWORDS: *doxorubicin, pH-responsive, photodynamic therapy, phthalocyanine, photosensitizer, tumor targeting*

INTRODUCTION

Photodynamic therapy (PDT) is an emerging noninvasive approach to skin and cavity diseases, and some malignant tumors.[1-3] In PDT, light-activating photosensitizers can pass on their excess energy to surrounding molecular oxygen to produce reactive oxygen species (ROS), such as free radicals and singlet oxygen ($^1O_2$) that are toxic to cells and tissues.[4-6] Generally, the major administration route of photosensitizers is intravenous (i.v.) injection. However, the clinically applied systemic photosensitizers combining with the long-term exposure to light radiation could lead to severe side effects, such as hepatotoxicity, renal toxicity, hypertension, hyperlipidemia, and skin cancers.[7]

Anticancer nanocarriers are fascinating due to their tumor targeting and environmental triggered drug release.[8] Nanocarriers are also introduced to deliver anticancer photosensitizers to obtain tumor targeting.[9-13] Furthermore, scientists are trying to combine chemotherapy and PDT for the treatment of cancer. Generally, a nanocarrier is used for entrapping both anticancer agents and photosensitizers.[14-16] Additionally, anticancer agents were covalently conjugated with photosensitizers, such as the conjugate of sulfonated aluminum phthalocyanine and doxorubicin (DOX),[17] and the conjugate of silicon phthalocyanine and paclitaxel.[18]

As a matter of fact, a photosensitizer does not need to be released into the surroundings because it is only the resource of singlet oxygen under lighting. Here, we designed a novel photosensitizer-core polymer as the drug-loaded nanocarrier, i.e., the photosensitizer is one part of the nanocarrier. Moreover, some functional groups

are induced into the polymer. The novel functional copolymer consists of zinc phthalocyanine as the core and a sequentially conjugated hydrophobic chain/pH-responsive chain/hydrophilic chain to form a four-armed star-shaped copolymer (Figure 1). When a drug (e.g., DOX) is entrapped in this copolymer, we call it a doxorubicin-loaded photosensitizer-core pH-responsive copolymer nanocarrier. The copolymer itself is a photosensitizer for PDT, and the entrapped DOX is released in a pH-dependent manner after targeting tumors (Figure 1). Our previous research has showed a drug-loaded star-shaped pH-responsive monomolecular copolymer nanocarriers for tumor targeting and cancer therapy.[19] We demonstrated that the tetra-(methoxy-poly(ethylene glycol)-poly(2-(N,N-diethylamino)ethyl methacrylate)-poly(ε-caprolactone) pentaerythritol ((mPEG-pDEA-PCL)$_4$-PET, PDCP) nanocarriers could be used to deliver hydrophobic anticancer drugs for cancer therapy with tumor targeting and controlled drug release. In this study, we replaced the pentaerythritol core with a zinc phthalocyanine core that is a photosensitizer while using the modified copolymer to load an anticancer drug.

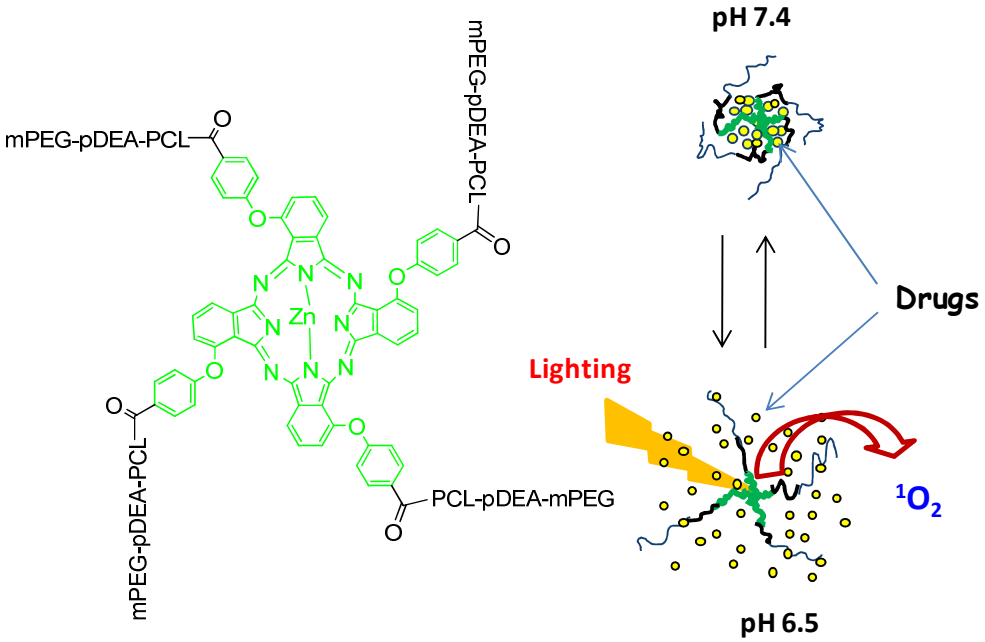

Figure 1. Molecular structure of PDCZP and illustration of its pH-dependent drug release and combined therapy of chemotherapy and photodynamic therapy.

EXPERIMENTAL SECTION

Materials. Doxorubicin (DOX) chloride was a gift from Zhejiang Hisun Pharmaceutical Co., Ltd., China. ε-Caprolactone (CL) was purchased from Aladdin, China. Tinoctoate ($Sn(Oct)_2$) was purchased from Sigma. Organic solvents were of analytical grade and other chemicals were of reagent grade. 9,10-Dimethylanthracene (DMA) was from TCI (Tokyo, Japan). Zinc phthalocyanine (ZnPc) from TCI was used as the control in the determination of singlet oxygen quantum yield. Purified water was prepared using Heal Force Super NW Water System (Shanghai Canrex Analytic Instrument Co., Ltd., Shanghai, China). The molecular weight cut-off of dialysis bags was from Union Carbide Corporation, New Jersey, USA. Ultraviolet–

visible (UV–vis) spectra, infrared (IR) spectra, and nuclear magnetic resonance (NMR) spectra were recorded on a Purkinje TU-1901 spectrophotometer (Beijing Purkinje General Instrument Co., Ltd., Beijing, China), a Bio-Rad FTS-65A infrared ray spectrometer, and a JNM-ECA-400 NMR spectrometer, respectively.

Animals. Healthy female Kunming mice (18-22 g) were from the Laboratory Animal Center of Beijing Institute of Radiation Medicine (BIRM). The animals were handled and surgically treated in strictly accordance with the Guidelines for the Use of Laboratory Animals. All the studies were conducted in accordance with the National Institutes of Health Guide for the Care and Use of Laboratory animals. The animal experiments were approved by the Animal Care Committee of BIRM.

Synthesis of PDCZP. The synthetic route of (mPEG-pDEA-PCL)$_4$-ZnPC$_4$ (PDCZP) is shown in Figure 2. mPEG was methoxy-poly(ethylene glycol) 2000 (Acros, Belgium). mPEG-pDEA-N_3 was synthesized in our lab according to our previous research.[20] The propargyl-terminated PCL was obtained by ring-opening polymerization of ε-CL under the co-initiation of propargyl alcohol and Sn(Oct)$_2$.[21] The polymerization was performed in a glovebox with a water content of less than 0.1 ppm. Propargyl alcohol (1.15 ml, 0.02 mol) and ε-CL (21.3 ml, 0.2 mol) were added to freshly dried toluene (20 ml) in a flask. Sn(Oct)$_2$ (0.12 g) was added and the solution was stirred at 80 °C for 12 h. The mixture was concentrated under vacuum. After precipitation in cold diethyl ether, the polymer was obtained and dried under vacuum overnight. Click reaction was used to prepare PDC.[22] The

propargyl-terminated PCL (1 g) and mPEG-pDEA-N_3 (1.5 g) were dissolved in tetrahydrofuran (THF, 20 ml). CuI (0.005 g) and 1,8-diazabicyclo[5.4.0]undec-7-ene (DBU) (0.18 ml) were added. The solution was stirred in a nitrogen-filled sealed flask at 60 °C for 24 h before being passed through a neutral alumina column to remove the copper catalyst. The solvent was removed to obtain a viscous liquid that was then dialyzed against water using a dialysis bag (cut-off MW, 7000) for 72 h. The solution in the bag was lyophilized to obtain a white solid of PDC. Infrared IR (KBr) ν_{max} (cm^{-1}): 2967, 2872 (-CH_2-), 1726 (-C=O-), 1113 (-C-O-C-), 1461 (-CH_2-). The absorption peak of azide group disappeared completely after the click reaction. Meanwhile, a strong absorption at 1726 cm^{-1} contributing to the C=O stretching of PCL block was observed. ^{1}H NMR (DMSO-d_6, 400 MHz) δ (ppm): 3.66 (pDEA, -CH_2-O-), 2.65 (pDEA, -CH_2-N-), 4.0 (mPEG, -CH_2-), 3.38 (mPEG, CH_3-O-), 2.35 (PCL，-CH_2-), 3.65 (PCL, –OH), 5.32 (-CH_2O-CO-), 7.80 (-NCH-).

The possible polymerization degrees in the molecule of $mPEG_m$-$pDEA_n$-PCL_l (PDC) may be accessed from the comprehensive structural information. The MALDI-TOF mass spectrum of mPEG-pDEA-Br showed the peaks of 2347, 4105, and 6055 m/z (Figure S1 in the Supporting Information), which belonged to mPEG, pDEA, and mPEG-pDEA-Br, respectively. According to the molecular structure, the polymerization degree of PEG, i.e., m, was about 53, and that of pDEA, i.e., n, was about 12. According to the ^{1}H NMR spectrum of propargyl-terminated PCL (Figure S2), the peak integral of 2-site H (δ, 2.31 ppm) of PCL units was 19 times of that of propargyl H (δ, 4.68 ppm), indicating that the polymerization degree of PCL was

about 19. Therefore, the polymerization degrees in mPEG-pDEA-PCL were possibly 53 (m), 12 (n), and 19 (l), respectively.

$ZnPC_4$ was prepared according to our previous research.[23] $ZnPC_4$ (1.13 g, 1 mmol) and PDC (5.03 g) were dissolved in THF (15 ml) by turns. DCC (0.307 g, 1.5 mmol) and N,N'-dimethylaminopyridine (DMAP, 0.121 g, 0.99 mmol) were added and then agitated at room temperature for 48 h. The solution was evaporated under vacuum until ca. 1 ml and then purified on a silica column with THF as the eluent. The green filtrate was dialyzed against water using a dialysis bag (cut-off MW, 8000-14000) for 72 h and refreshing water every 3 h. The solution in the bag was lyophilized to obtain a green solid of PDCZP. UV-vis (THF): λ_{max} = 348, 681 nm; IR (KBr) ν_{max} (cm^{-1}): 732.1 (Zn-N), 1088.4, 1504.5, 1601.1, 1627.0 (phthalocyanine), 1241.6 (Ar-O-Ar), 1726.8 (-CO-), 2853.3 ($-CH_2-$); ^1H NMR (DMSO-d_6, 400 MHz) δ (ppm): 1.5 (m, Pc-Pc), 2.25 (m, PCL, $-CH_2-$), 4.0 (m, PEG, $-CH_2-$), 3.5 (m, pDEA, $-CH_2-O-$), 2.5 (m, pDEA, $-CH_2-N-$), 5.3 (d, $-CH_2-CO-$), 7.0-7.8 (m, H-phthalocyanine), 8.0 (m, H-Ar).

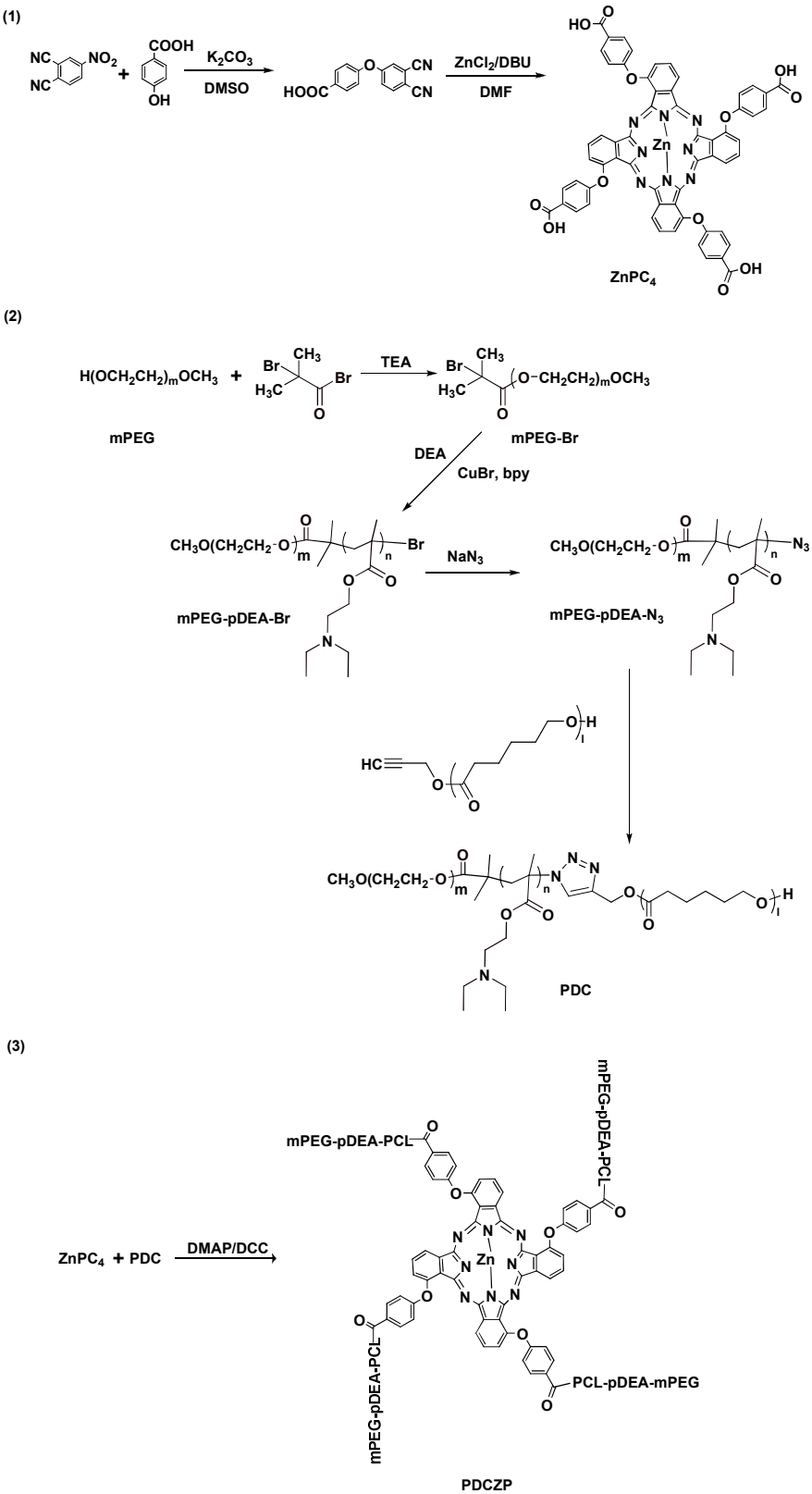

Figure 2. Synthetic routes of PDCZP.

Preparation and Characterization of PDCZP Nanocarriers. A PDCZP solution (2 mg/ml) in THF was prepared. The solution was injected into water using a microsyringe under bath sonication until a homogenous green suspension was obtained. THF was removed from the suspension under vacuum at 37 °C for 5 min followed by evaporation at room temperature. The DOX-loaded PDCZP nanocarriers were prepared using a similar method to the one mentioned above. DOX chloride was first neutralized with triethylamine (1:3, mol/mol) in a little acetone and then mixed with a PDCZP solution in THF at a series of DOX/PDCZP ratios (1:2, 1:5, 1:10, 1:20, w/w). The mixed solutions were separately injected in water followed by removal of solvents as mentioned above to obtain a homogenous, nearly transparent, and green suspension that could be further concentrated following removal of some water or directly lyophilized to powders.

The THF solutions of ZnPc, $ZnPC_4$, and PDCZP were UV-vis scanned in the range of 200 to 800 nm, respectively. PDCZP nanocarriers were observed under a Hitachi H-7650 80-kV transmission electron microscope (TEM) after staining with a sodium phosphotungstate solution (pH 7.4) as reported previously.[24] A dynamic lighting scattering (DLS) method on Zetasizer Nano ZS (Malvern, UK) was applied to measure the sizes of PDCZP nanocarriers at different pH. The zeta potentials of PDCP nanocarriers were also measured with the above instrument at 25 °C.

Determination of DOX. The DOX-loaded PDCZP nanocarriers were separated from the suspension by centrifuging through an ultrafiltration tube (cut-off MW,

10000, PALL Corporation, USA) at 5000× g for 10 min. The nanocarriers remained above the ultrafiltration membrane, while free DOX existed in the filtrate. DOX was analyzed using the high performance liquid chromatography (HPLC), involving a system of LC-10Avp series (Shimadzu, Japan), a Tianhe® ODS-C18 column (150 mm × 4.6 mm, 10 μm) at 30 °C, a mobile phase of methanol/20 mM ammonium acetate/acetic acid (60:40:5.4, v/v) with a flow rate of 0.8 ml/min, and a detection wavelength of 254 nm. The drug encapsulation efficiency (EE) and drug loading efficiency (DL) were calculated as Eq. (1) and (2).

$$EE = \frac{W_{D1}}{W_{D2}} \times 100\% \quad (1)$$

$$DL = \frac{W_{D1}}{W_{PDPZP} + W_{D1}} \times 100\% \quad (2)$$

where W_{D1} was the DOX content in the nanocarriers, W_{D2} was the total added drug content, W_{PDCZP} was the added copolymer content.

Drug Release from PDCZP Nanocarriers. A dialysis method was used to evaluate drug release from PDCZP nanocarriers. The DOX-loaded PDCZP suspension (2 ml) was put into a dialysis bag (cut-off MW, 3500) and dialyzed against the media (50 ml) in an oscillating incubator (120 rpm, 37 °C). Aliquots (1 ml) of the buffered solutions were collected at the predetermined time points and then supplemented with the same volume of media. The released drug was determined using the above HPLC method and the cumulative release was calculated. The dialysis media were phosphate buffered solutions (PBS, pH 5.0, 6.5, or 7.4).

Determination of Singlet Oxygen Quantum Yield of PDCZP. Determination of singlet oxygen quantum yield was performed according to our previous report.[23] The test was based on the changes of a singlet oxygen chemical quencher DMA in DMF. The stock solutions of ZnPc, DMA and PDCZP in DMF were prepared. The solutions of ZnPc (3 μM), PDCZP (3 μM), DMA (90 μM), ZnPc (3 μM)/DMA (90 μM), PDCZP (3 μM)/DMA (90 μM) were obtained after dilution and/or mixing of the stock solutions with DMF. A 100-mW 657-nm laser emitter (YSHINELASER, China) was used to excite the solutions (each aliquot of 3 ml) of photosensitizers in the 1-cm cuvette through a 9-mm diameter hole. The laser radiation process was performed under dark conditions. The light intensity was determined as 8.12 mW/cm^2 with Nova II (OPHIR, Israel). The absorbance of the radiated solutions at 405 nm was measured on the UV-vis spectrophotometer every 30 s. The eliminated DMA rate constants (K_{DMA}) were obtained as Eq. (3).

$$\ln\frac{A_0}{A_t} = K_{DMA}t \qquad (3)$$

where A_0 was the initial absorbance of DMA-contained solutions without laser radiation, while A_t was the absorbance of solutions at t time. The absorbance of DMA solutions was also measured in the same time range as above to confirm that DMA was not oxidized by the oxygen in the atmosphere. DMA oxidation was used to determine the singlet molecular oxygen ($^1O_2$) produced by the photosensitizers.

The photon absorption rate constants (K_{pho}) of photosensitizers were calculated using Eq. (4).

$$K_{pho} = \frac{0.97 \times P \times (1 - 10^{-AL})}{(0.1197/\lambda) \times V} \quad (4)$$

where P was the light intensity (8.12 mW/cm^2), A was the absorbance of photosensitizer solutions at the laser wavelength (657 nm), V was the volume of solutions (3 ml), L was the light length on the solutions (1 cm), λ was the light length (657 nm), and the value of 0.97 was the correct factor of the reflecting light at the interface of air/glass. Singlet oxygen quantum yields (Φ) of photosensitizers were the direct ratios of DMA oxidation rate. The Φ_{ZnPc} of ZnPc in DMF was 0.56 [25]. Therefore, the Φ_{PDCZP} can be calculated as Eq. (5).

$$\frac{\Phi_{PDCZP}}{\Phi_{ZnPc}} = \frac{(K_{DMA}/K_{pho})_{PDCZP}}{(K_{DMA}/K_{pho})_{ZnPc}} \quad (5)$$

Cytotoxicity Test. DOX chloride solutions, PDCZP suspensions, and DOX-loaded PDCZP suspensions were sterilized with ^{60}Co γ-ray radiation. Cytotoxic experiments were performed on human breast cancer MCF-7 cells, human colon cancer SW480 cells, and human hepatocellular cancer HepG2 cells. The cells were cultured in a DMEM supplemented with 10% fetal bovine serum (FBS) at 37 °C. The cells were seeded in the 96-well plates with 2000 cells/well to adhere to the plates thoroughly. Four hours after incubation in the dark, the plates were exposed under a fluorescent lamp with the light intensity of 4500 Lx for 30 min, and then incubated for 24 h. Aliquots (20 μl) of MTT solutions were separately added to each well and the cells were further incubated for 5 h. The media were subsequently collected and dimethyl sulphoxide (DMSO, 150 μl) was added to dissolve the dark-blue formazan crystals. Formazan was measured at 490 nm using a microplate reader (Multiskan MK3，

Thermo Scientific, US). Cell viability was calculated as (absorbance of experimental groups)/(absorbance of negative control)×100%. The half concentration of inhibition (IC_{50}) was then deduced.

Hemolysis Assay. Rat erythrocyte suspensions (2%, v/v) in saline were prepared according to the report.[26] A series of samples were prepared, containing 1% erythrocytes and a series of PDCZP suspensions in saline and they were incubated at 37 °C until observation. Hemolysis was observed with naked eyes against the completely hemolytic sample of water-mixed erythrocytes. Four hours later, the supernatants were also collected and measured with the spectrophotometry at 577 nm.

Tumor Implantation. A murine hepatoma H_{22} cancer cell line was used. H_{22} cancer cells were extracted from the abdominal dropsy of mice bearing cancer cells and diluted with saline to achieve a concentration of 3×10^7 cells/ml. Aliquots (0.2 ml) of the cell suspensions were separately and subcutaneously (s.c.) injected into the mice under the right forelimb. Five days after transplant, the injected mice of appropriate tumor volumes were selected for tissue distribution and pharmacodynamic studies.

Pharmacodynamic Study. Thirty mice with the expected tumor volume were equally divided into six groups: (A) the saline group treated with saline; (B) the blank PDCZP group treated with PDCZP/dark; (C) the light group just with lighting alone; (D) the PDCZP/light group treated with PDCZP/lighting; (E) the DOX-loaded PDCZP group treated with DOX-loaded PDCZP/dark; (F) the DOX-loaded

PDCZP/light group treated with DOX-loaded PDCZP/lighting. PDCZP solution had 0.68 mg PDCZP/ml. DOX-loaded PDCZP solution had 207 μM DOX and 0.78 mg PDCZP/ml. The dose was 3 mg DOX/kg for Group E and F, and 17 mg PDCZP/kg for Group B and D. Aliquots (0.5 ml) of the medicines were i.v. injected to the mice via the tail veins once every two days totally for 3 times. All the animals were housed under dark conditions unless they were treated with a laser light. After injection, the mice were raised for 12 h under dark conditions and the groups of C, D, and F were lighted on the tumor xenografts for 15 min using a large He-Ne laser lighter (JK-3, equipped in BIRM).

Xenograft sizes were measured in two perpendicular dimensions using a caliper once a day after treatment. The first administration day was recorded as Day 1. Tumor volume (V) was calculated as $0.5L\times W^2$, where L was the largest superficial diameter, and W was the smallest superficial diameter of the xenograft. Six 6 days later, the mice were sacrificed. Tumors were taken and weighed to calculate the tumor inhibitory rates as Eq. (6).

$$\text{Tumor inhibitory rate}\,(\%) = \frac{W_{blank} - W_{test}}{W_{blank}} \times 100\% \qquad (6)$$

where W_{blank} and W_{test} were the average tumor weight of the control group and the test groups, respectively. Mice were weighed daily.

All the results were expressed as mean±standard deviation (SD). Student's t-test was used for comparison of the two means. A significance level of $p < 0.05$ and $p < 0.01$ represented statistical difference and significant difference, respectively.

Fluorescence Non-Invasively Tumor Imaging. A DOX-loaded PDCZP solution of 207 μM DOX and 0.78 mg PDCZP/ml was used. It was i.v. injected into the H_{22} tumor-bearing mice via tail veins at the dose of DOX 10 mg/kg. The mice were sacrificed. The organs, including the heart, liver, spleen, lung, kidney, and tumor, were immediately surgically isolated at 0.5, 1, 2, 4 and 8 h after administration, respectively. The organs were washed with saline and immersed in formalin before imaging. The organs were moved to the imaging chamber for scanning. Excitation and emission spots were raster-scanned in 1 mm steps to generate emission wavelength scans. A 675 nm pulsed laser diode was used to excite PDCZP without exciting the tissue matrix and fluorescence interference. The organs were imaged on an imaging system (NightOWL II LB 983, Germany) and a cold CCD fluorescence/illuminating tissues imaging system (LB983-NC100, Berphold, Germany).

RESULTS AND DISCUSSION

Formation of the Drug-Loaded Photosensitizer-Core Nanocarrier. The preparation of the nanocarriers was simple, i.e., injecting its THF solution into water under bath sonication. THF was a good solvent of PDCZP and easily removed under vacuum, which was why it was selected. In this study, the loaded drug, i.e., DOX, was easily entrapped into the large intra-space of PDCZP nanocarriers using the similar process as above, wherein the alkalized DOX was dissolved in THF with PDCZP. The 1:10 (w/w) ratio of DOX/PDCZP was used after screening. The drug

encapsulation efficiency (EE) and drug loading efficiency (DL) were 94.3% and 14.46%, respectively. A homogenously transparent green solution was obtained.

Properties of the Nanocarriers. PDCZP nanocarriers showed different sizes and zeta potentials depending on pH (Figure 3A-D). The carriers changed from small at high pH to large at low pH with the size of 51, 105, and 342 nm at pH 7.4, 6.5, and 5.0, respectively. The zeta potential was gradually increased from 7.15, 16.2, to 26.1 mV at the above pH, respectively. The TEM images also showed a similar result (Figure 3A-C). The >300 nm sizes and the significant size changes indicated the supramolecular assemblies of PDCZP could be formed in the nanocarriers. However, the strong pH dependency of PDCZP nanocarriers was confirmed. Because of the small size, PDCZP nanocarriers could easily enter tumor tissues from the circulation based on the enhanced permeability and retention (EPR) effect.[27] PDCZP nanocarriers might be stable because no significant precipitates appeared within one month. The outside PEG chains of PDCZP could produce the space static effect to prevent the aggregation of nanocarriers.[28]

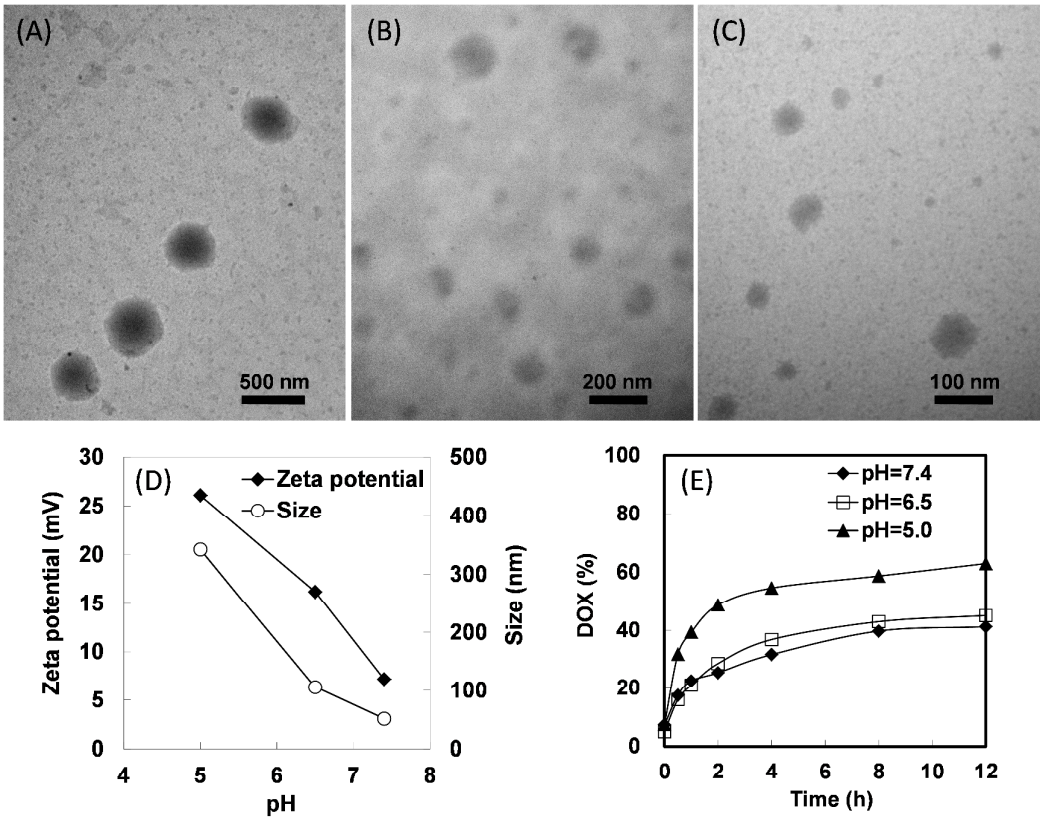

Figure 3. Properties of PDCZP nanocarriers. TEM images at pH 5.0 (A), pH 6.5 (B), and pH 7.4 (C). Size and zeta potential profiles at different pH (D). DOX release profiles of DOX-loaded PDCZP at different pH (E).

PDCZP and $ZnPC_4$ showed two UV-vis absorption peaks at 354 nm and 677 nm. The conventional phthalocyanine, i.e., ZnPc, has two absorption peaks at 342 nm and 669 nm (Figure S3). The red shifts of PDCZP and $ZnPC_4$ absorption may be attributed to the four-carboxyl derivation of ZnPc. More importantly, the light of long wavelengths can penetrate through biological tissues into the deep sites better than the light of short wavelengths.[30]

PDCZP did not show hemolysis within 3 h after incubation with erythrocytes even when PDCZP concentration was up to 5 mg/ml. Moreover, four hours post-incubation, the supernatants of a series of samples did not show hemolysis because the absorbances were close to zero. Therefore, the i.v. injected PDCZP was safe.

pH-Dependent Drug Release from the Nanocarriers. PDCZP is a pH-responsive nanocarrier, resulting from the pH-responsive pDEA chain. pDEA is poly(2-(N,N-diethylamino)ethyl methacrylate), occupying one tertiary amine group in its monomer. The pDEA chains could shrink in weakly basic environments (such as pH 7.4 in the circulation) due to the hydrophobic form. However, the chains could extend in weakly acidic environments (such as pH 6.5 in the tumor microenvironment or 5.0 in the endosomes) because the amines of pDEA transformed into the protonized forms that were hydrophilic. Our previous research on the pDEA-composed co-polymers also showed similar results.[19, 20, 31] The pH-responsive function of PDCZP could make it open at low pH and close at high pH. Therefore, simply switching the pH of media can be used for entrapping or releasing the cargos in PDCZP. In this study, the release of DOX from the PDCZP nanocarriers was significantly pH-dependent and was accelerated as pH decreased (Figure 3B). Furthermore, we predicted that DOX would remain in PDCZP nanocarriers when circulating in the blood (pH 7.4), and release itself when reaching tumor tissues or entering the endosomes.[19]

Photodynamic Effect of Nanocarriers. Singlet oxygen quantum yield (Φ) is a key parameter of photosensitizers. High Φ values indicate high production of ROS. The Φ of PDCZP was 0.41, a little lower than the values of parent ZnPc (0.56) and another amphiphilic derivative of ZnPc (ZnPc-Brij 58 conjugate, ZPB, 0.64) previously prepared in our lab.[23] The long PDC chains of PDCZP might shield energy transportation or oxygen diffusion, leading to decrease of the Φ value.

Cytotoxicity of DOX-Loaded Nanocarrier. Three types of cancer cell lines were used for detecting the *in vitro* anticancer effects of DOX, PDCZP, and DOX-loaded PDCZP. Cell viabilities were measured following addition of different medicines, respectively, and a 30-min lighting process with a fluorescent lamp. We found that lighting played a key role in the anticancer effect of PDCZP used alone or DOX-loaded PDCZP (Figure 4). The group of DOX-loaded PDCZP/light had a highest cytotoxicity than the other two groups, and the difference was statistically significant ($p < 0.01$). In addition, PDCZP did not show any cytotoxic effect on a melanoma cell line B16-F10 under dark conditions even at the high concentration of 100 μg/ml (Figure S4). Therefore, the photodynamic effect of PDCZP carriers was confirmed.

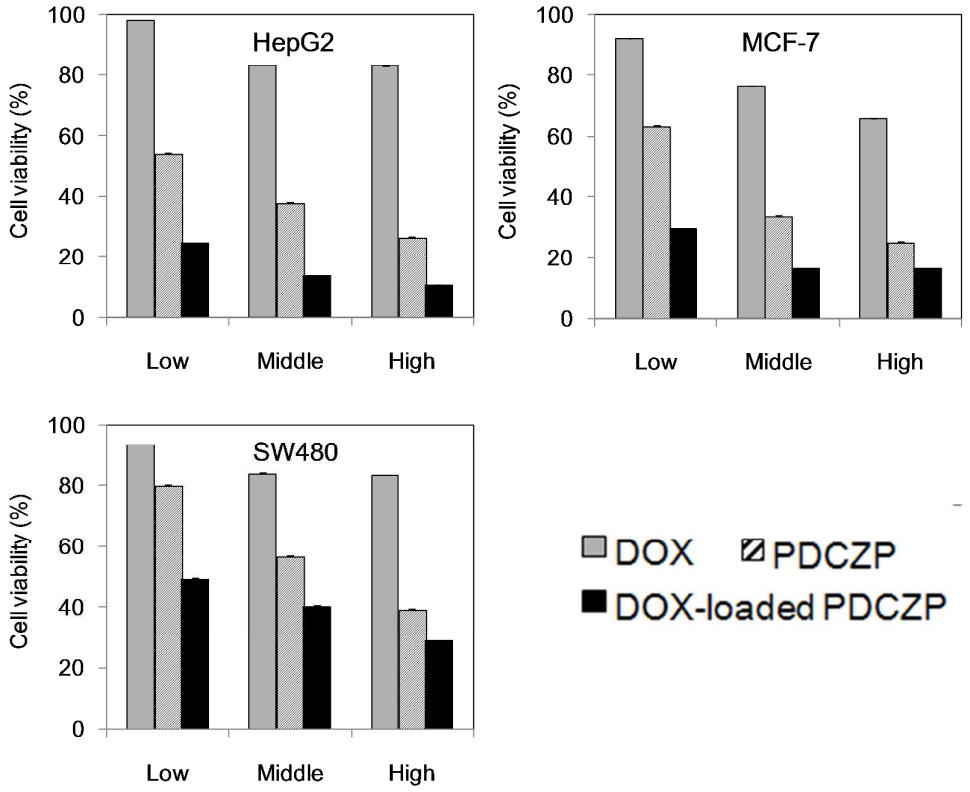

Figure 4. Cytotoxicity of DOX, PDCZP, and DOX-loaded PDCZP on the cancer cell lines, including HepG2, MCF-7, and SW480, respectively. "Low", "Middle", and "High" indicate the concentration levels of DOX (13.0, 31.1, 60.3 μM), PDCZP (40, 100, 200 μg/ml), and DOX-loaded PDCZP (DOX at 13.2, 31.8, 63.6 μM, and PDCZP at 50, 120, 240 μg/ml), respectively. All the data are presented as means ± SD (n=6).

Anticancer Effect of DOX-Loaded Nanocarrier. The murine hepatocellular carcinoma (H22)-bearing mice were i.v. administrated with saline, PDCZP, and DOX-loaded PDCZP, respectively, once every two days. Twelve hours after injection, the mice were exposed to laser lighting for 15 min or chronically under dark conditions. On the second day after the final administration, the mice were sacrificed. In this study, free DOX solutions were also injected to the mice which, however,

showed little movement, dull hair, and twitch from Day 3. Finally, some mice died from the serious side effect, which should be attributed to the strong heart toxicity of free DOX.[31] In contrast, no mice died in the other groups. It is known that free DOX shows strong heart toxicity.[32] In our previous research, free DOX solutions were also demonstrated to have serious toxicity on healthy mice. However, DOX-loaded nanocarriers decreased the toxicity due to the low distribution in the heart.[9] Therefore, a nanoscale formulation, i.e., liposomal DOX, becomes a major alternative of DOX solutions in clinics.

Both PDCZP/light and DOX-loaded PDCZP/light showed good anticancer effects according to the tumor volume (Figure 5A). Furthermore, the group of DOX-loaded PDCZP/light had the lowest mean tumor weight. Interestingly, the dark/light groups of the same medicines showed statistical differences in tumor weight with $p < 0.05$ (PDCZP under dark *vs.* lighting) and $p < 0.01$ (DOX-loaded PDCZP under dark vs. lighting). The tumor inhibitory rate was 67.60% in the DOX-loaded PDCZP/light group, but was 27.77%, 54.92%, and 28.06% in the other groups, including the PDCZP/dark group, the PDCZP/light group, and the DOX-loaded PDCZP/dark group. We noted that tumor inhibition was mild in the PDCZP/dark group. PDCZP is a large copolymer, composed of mPEG, pDEA, PCL, $ZnPC_4$ moieties, where ester bonds dominate. Therefore, it would finally be degraded *in vivo* and excreted to urine though the process of degradation might be slow. Some unknown mechanisms might have led to the systemic toxicity because the animal body weight of the PDCZP/dark group decreased, which further led to tumor weight decrease. The DOX-PDCZP/dark

group also showed a similar result. Fortunately, the DOX-PDCZP/light group showed smaller tumors and higher body weight. Cancer is a complicated disease where tumor growth, body weight, and systemic toxicity are mutually related. Therefore, the combinatorial therapy using the DOX-loaded photosensitizer-core nanocarriers could be a perfect method with high anticancer effect and very weak side effect.

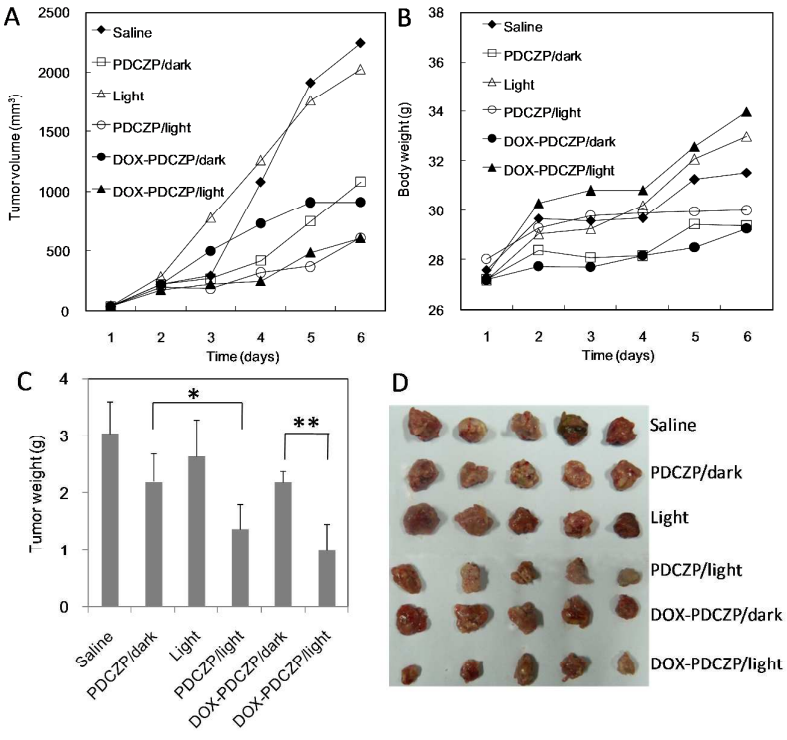

Figure 5. Anticancer effects of different medicines under dark conditions or lighting on the H22 tumor-bearing mice. Tumor volume profiles (A). Body weight profiles (B). Tumor weight after treatments (C). * $p < 0.05$; ** $p < 0.01$. (D) Tumors after treatments. All the data are presented as means ± SD (n=5).

Tumor Targeting of the Nanocarriers. We detected the tumor targeting effect of PDCZP using the fluorescence non-invasively tumor imaging method. Besides the

photodynamic effect, PDCZP has the fluorescent function for imaging *in vivo*. The imaging results showed that the distribution of DOX-loaded PDCZP into the organs was slow, which may be attributed to the long-circulating effect of PDCZP due to its long hydrophilic chains (Figure 6). Two hours post-administration, PDCZP reached the maximal level in the liver. And then, PDCZP in the liver decreased and increased in the heart, kidney and tumor. Eight hours later, PDCZP reached the maximal levels in the kidney and tumor. Hence, the tumor targeting of PDCZP was confirmed. PDCZP or its metabolites could be eliminated from the major distributed tissues (e.g, the liver) to the blood. And they would finally be excreted into urine. Cationic small nanoparticles are also readily excreted into urine after injection.[33] Therefore, PDCZP could not accumulate in the organs, and only to be eliminated from the body.

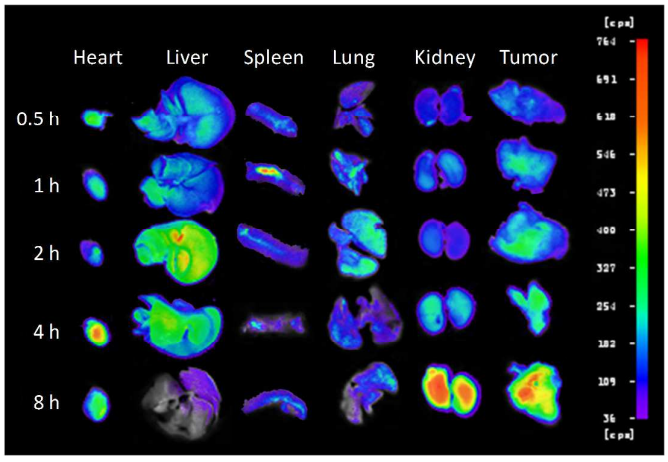

Figure 6. Fluorescence non-invasively tumor imaging after injecting the DOX-loaded PDCZP to the tumor-bearing mice.

CONCLUSIONS

A doxorubicin-loaded photosensitizer-core pH-responsive star-shaped copolymer nanocarrier was prepared in this study. The unique advantage of this nanocarrier is the simultaneous work of chemotherapy and PDT. We demonstrated that one case of this functional nanocarrier, i.e., the DOX-loaded PDCZP, showed pH-responsive drug release, high anticancer effect, and tumor targeting effect. The photosensitizer-core nanocarrier is a promising photodynamic nanocarrier that can be integrated with other therapies.

ASSOCIATED CONTENT

Supporting Information

The Supporting Information is available free of charge on the ACS Publications website at DOI: 10.1021/

MALDI-TOF mass spectrum of mPEG-pDEA-Br, ^{1}H NMR spectrum of propargyl-terminated PCL, UV spectra of ZnPc, $ZnPC_4$, and PDCZP, cell viability of PDCZP on B16-F10 cells under dark conditions.

AUTHOR INFORMATION

Corresponding Author

*E-mail: jinyg@sina.com

Notes

The authors declare no competing financial interest.

ACKNOWLEDGEMENTS

We are grateful for the support from the National Natural Science Foundation of China (No. 81373340). We thank Prof. Shoujun Yuan for providing all the cancer cell lines, and Prof. Xiansheng Lu for Language editing and proof-reading.

REFERENCES

(1) Celli, J. P.; Spring, B. Q.; Rizvi, I.; Evans, C. L.; Samkoe, K. S.; Verma, S.; Pogue, B. W.; Hasan, T., Imaging and photodynamic therapy: Mechanisms, monitoring, and optimization. *Chem. Rev.* **2010,** 110, 2795-2838.

(2) Hong, E. J.; Choi, D. G.; Shim, M. S., Targeted and effective photodynamic therapy for cancer using functionalized nanomaterials. *Acta Pharm. Sin. B* **2016,** 6, 297-307.

(3) Pradhan, M.; Singh, D.; Singh, M. R., Novel colloidal carriers for psoriasis: Current issues, mechanistic insight and novel delivery approaches. *J. Control. Release* **2013,** 170, 380-395.

(4) Ohulchanskyy, T. Y.; Roy, I.; Goswami, L. N.; Chen, Y.; Bergey, E. J.; Pandey, R. K.; Oseroff, A. R.; Prasad, P. N., Organically modified silica nanoparticles with covalently incorporated photosensitizer for photodynamic therapy of cancer. *Nano Lett.* **2007,** 7, 2835-2842.

(5) Mackowiak, S. A.; Schmidt, A.; Weiss, V.; Argyo, C.; von Schirnding, C.; Bein,

T.; Bräuchle, C., Targeted drug delivery in cancer cells with red-light photoactivated mesoporous silica nanoparticles. *Nano Lett.* **2013,** 13, 2576-2583.

(6) Oniszczuk, A.; Wojtunik-Kulesza, K. A.; Oniszczuk, T.; Kasprzak, K., The potential of photodynamic therapy (pdt)—experimental investigations and clinical use. *Biomed. Pharmacother.* **2016,** 83, 912-929.

(7) Richard, E. G.; Hönigsmann, H., Phototherapy, psoriasis, and the age of biologics. *Photodermatol. Photoimmunol. Photomed.* **2014,** 30, 3-7.

(8) Duan, X.; Chen, H.; Fan, L.; Kong, J., Drug self-assembled delivery system with dual responsiveness for cancer chemotherapy. *ACS Biomater. Sci. Eng.* **2016,** 2016, 2347-2354.

(9) Li, Y.; Lin, T.-y.; Luo, Y.; Liu, Q.; Xiao, W.; Guo, W.; Lac, D.; Zhang, H.; Feng, C.; Wachsmann-Hogiu, S.; Walton, J. H.; Cherry, S. R.; Rowland, D. J.; Kukis, D.; Pan, C.; Lam, K. S., A smart and versatile theranostic nanomedicine platform based on nanoporphyrin. *Nat. Comm.* **2014,** 5, 4712.

(10) Master, A.; Malamas, A.; Solanki, R.; Clausen, D. M.; Eiseman, J. L.; Gupta, A. S., A cell-targeted photodynamic nanomedicine strategy for head and neck cancers. *Mol. Pharmaceut.* **2013,** 10, 1988-1997.

(11) Lee, S. J.; Koo, H.; Jeong, H.; Huh, M. S.; Choi, Y.; Jeong, S. Y.; Byun, Y.; Choi, K.; Kim, K.; Kwon, I. C., Comparative study of photosensitizer loaded and conjugated glycol chitosan nanoparticles for cancer therapy. *J. Control. Release* **2011,** 152, 21-29.

(12) Zhen, Z.; Tang, W.; Guo, C.; Chen, H.; Lin, X.; Liu, G.; Fei, B.; Chen, X.; Xu, B.;

Xie, J., Ferritin nanocages to encapsulate and deliver photosensitizers for efficient photodynamic therapy against cancer. *ACS Nano* **2013,** 7, 6988-6996.

(13) Ban, Q.; Bai, T.; Duan, X.; Kong, J., Noninvasive photothermal cancer therapy nanoplatforms via integrating nanomaterials and functional polymers. *Biomater. Sci.* **2017**, Doi: 10.1039/C6BM00600K

(14) Conte, C.; Ungaro, F.; Maglio, G.; Tirino, P.; Siracusano, G.; Sciortino, M. T.; Leone, N.; Palma, G.; Barbieri, A.; Arra, C.; Mazzaglia, A.; Quaglia, F., Biodegradable core-shell nanoassemblies for the delivery of docetaxel and zn(ii)-phthalocyanine inspired by combination therapy for cancer. *J. Control. Release* **2013,** 167, 40-52.

(15) Deng, X.; Chen, Y.; Cheng, Z.; Deng, K.; Ma, P.; Hou, Z.; Liu, B.; Huang, S.; Jin, D.; Lin, J., Rational design of a comprehensive cancer therapy platform using temperature-sensitive polymer grafted hollow gold nanospheres: Simultaneous chemo/photothermal/photodynamic therapy triggered by a 650 nm laser with enhanced anti-tumor efficacy. *Nanoscale* **2016,** 8, 6837-6850.

(16) Yue, C.; Zhang, C.; Alfranca, G.; Yang, Y.; Jiang, X.; Yang, Y.; Pan, F.; de la Fuente, J. M.; Cui, D., Near-infrared light triggered ros-activated theranostic platform based on ce6-cpt-ucnps for simultaneous fluorescence imaging and chemo-photodynamic combined therapy. *Theranostics* **2016,** 6, 456-469.

(17) Qin, Y.-L.; Huang, X.; Chen, J.-Y., Conjugation of sulfonated aluminum phthalocyanine to doxorubicin can improve the efficacy of photodynamic cancer therapy. *Anti-Cancer Drugs* **2012,** 23, 1047-1053.

(18) Thapa, P.; Li, M.; Bio, M.; Rajaputra, P.; Nkepang, G.; Sun, Y.; Woo, S.; You, Y., Far-red light-activatable prodrug of paclitaxel for the combined effects of photodynamic therapy and site-specific paclitaxel chemotherapy. *J. Med. Chem.* **2016,** 59, 3204-3214.

(19) Li, Q.; Jin, Y.; Li, M.; Dong, J.-X., Drug-loaded star-shaped ph-responsive monomolecular copolymer nanocarriers for tumor targeting and cancer therapy. *ACS Biomat. Sci. Eng.* **2015,** 1, 175-182.

(20) Du, L.; Jin, Y.; Yang, J.; Wang, S.; Wang, X., A functionalized poly(amidoamine) nanocarrier loading 5-fluorouracil: Ph-responsive drug release and enhanced anticancer effect. *Anti-Cancer Drugs* **2013,** 24, 172-180.

(21) Storey, R. F.; Sherman, J. W., Kinetics and mechanism of the stannous octoate-catalyzed bulk polymerization of epsilon-caprolactone. *Macromolecules* **2002,** 35, 1504-1516.

(22) Hartmuth, C. K.; Finn, M. G.; Sharpless, K. B., Click chemistry: Diverse chemical function from a few good reactions. *Angew. Chem. Int. Ed.* **2001,** 40, 2004-2021.

(23) Jin, Y.; Zhang, X.; Zhang, B.; Kang, H.; Du, L.; Li, M., Nanostructures of an amphiphilic zinc phthalocyanine polymer conjugate for photodynamic therapy of psoriasis. *Colloids Surf. B Biointerfaces* **2015,** 128, 405-409.

(24) Jin, Y.; Ren, X.; Wang, W.; Ke, L.; Ning, E.; Du, L.; Bradshaw, J., A 5-fluorouracil-loaded ph-responsive dendrimer nanocarrier for tumor targeting. *Int. J. Pharm.* **2011,** 420, 378-384.

(25) Cormick, M. P.; Rovera, M.; Durantini, E. N., Synthesis, spectroscopic properties and photodynamic activity of a novel zn(ii) phthalocyanine substituted by fluconazole groups. *J. Photochem. Photobiol. A Chem.* **2008,** 194, 220-229.

(26) Jin, Y.; Tong, L.; Ai, P.; Li, M.; Hou, X., Self-assembled drug delivery systems. 1. Properties and in vitro/in vivo behavior of acyclovir self-assembled nanoparticles (san). *Int. J. Pharm.* **2006,** 309, 199-207.

(27) Mitra, S.; Gaur, U.; Ghosh, P. C., Tumour targeted delivery of encapsulated dextran-doxorubicin conjugate using chitosan nanoparticles as carrier. *J. Control. Release* **2001,** 74, 317-323.

(28) Torchilin, V. P., Drug targeting. *Eur. J. Pharm. Sci.* **2000,** 11, S81-S91.

(29) Zhao, P.; Song, Y.; Dong, S.; Niu, L.; Zhang, F., Synthesis, photophysical and photochemical properties of amphiphilic carboxyl phthalocyanine oligomers. *Dalton Trans.* **2009,** 41, 6327-6334.

(30) Ghoroghchian, P. P.; Therien, M. J.; Hammer, D. A., In vivo fluorescence imaging: A personal perspective. *WIREs Nanomed. Nanobiotech.* **2009,** 1, 156-167.

(31) Jin, Y.; Ren, X.; Wang, W.; Ke, L.; Ning, E.; Du, L.; Bradshaw, J., A 5-fluorouracil-loaded ph-responsive dendrimer nanocarrier for tumor targeting. *Int. J. Pharm.* **2011,** 420, 378-384.

(32) Singal, P. K.; Iliskovic, N., Doxorubicin-induced cardiomyopathy. *N. Engl. J. Med.* **1998,** 339, 900-905.

(33) Liang, X.; Wang, H.; Zhu, Y.; Zhang, R.; Cogger, V. C.; Liu, X.; Xu, Z. P.; Grice, J. E.; Roberts, M. S., Short- and long-term tracking of anionic ultrasmall

nanoparticles in kidney. *ACS Nano* **2016,** 10, 387-395.

For Table of Contents Use Only

A Doxorubicin-Loaded Photosensitizer-Core pH-Responsive Copolymer Nanocarrier for Combining Photodynamic Therapy and Chemotherapy

Xiaohan Zhang, Qiu Li, Xiaodong Sun, Baolei Zhang, Hongxiang Kang, Fuli Zhang, and Yiguang Jin*

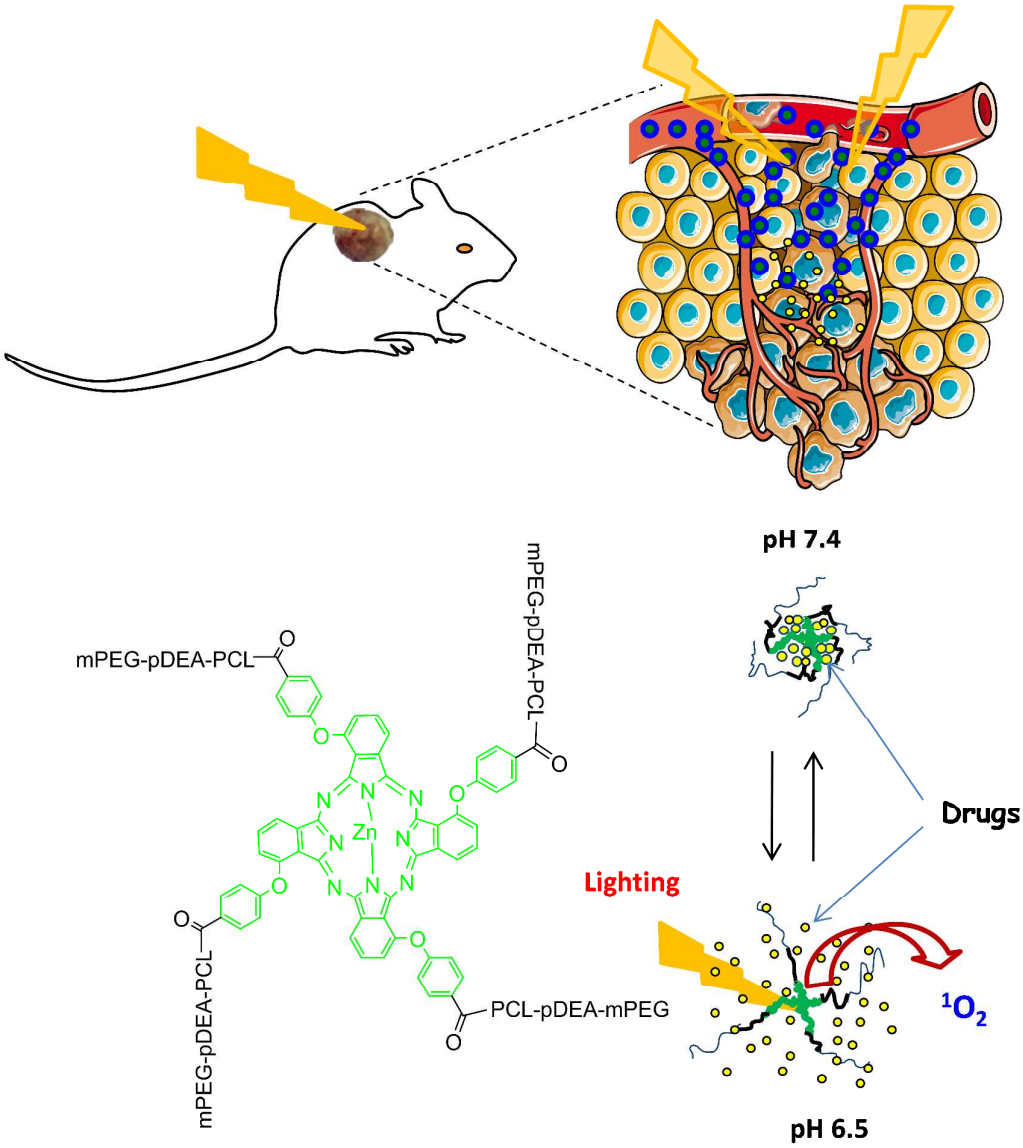

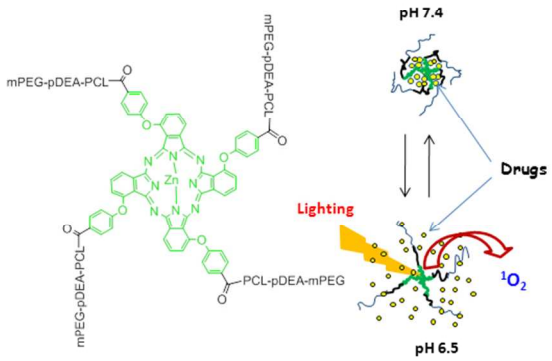

Figure 1. Molecular structure of PDCZP and the illustration of its pH-dependent drug release and combined therapy of chemotherapy and photodynamic therapy.
Figure 1
254x190mm (96 x 96 DPI)

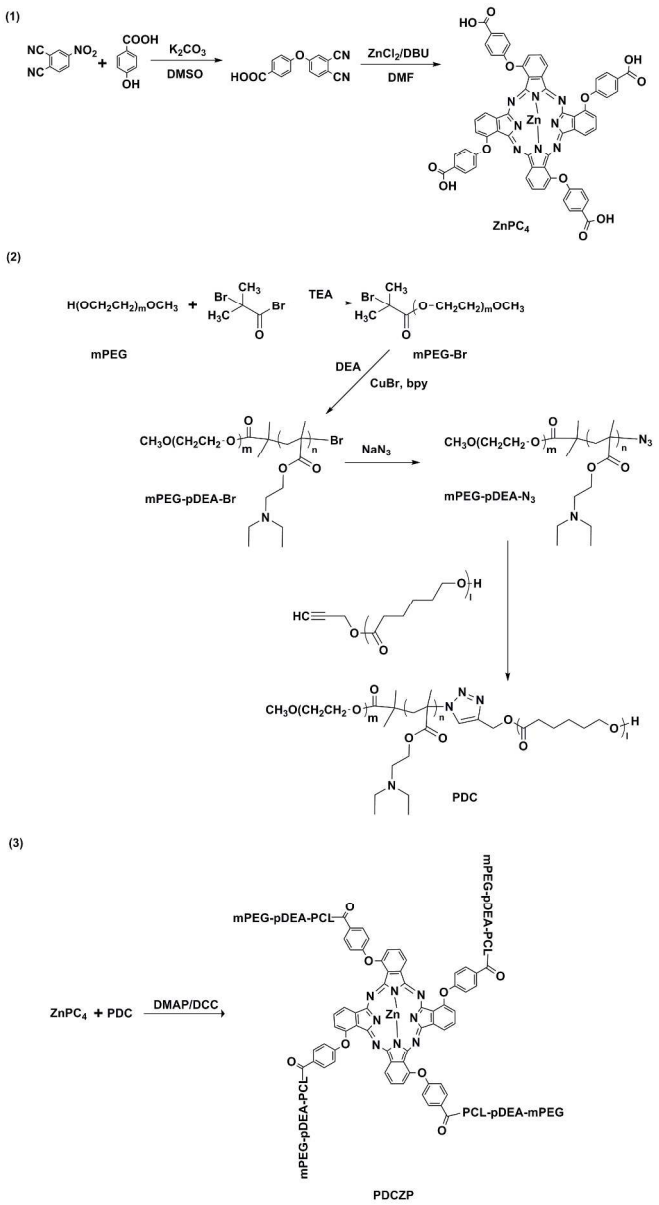

Figure 2. Synthetic routes of PDCZP.
Figure 2
170x312mm (300 x 300 DPI)

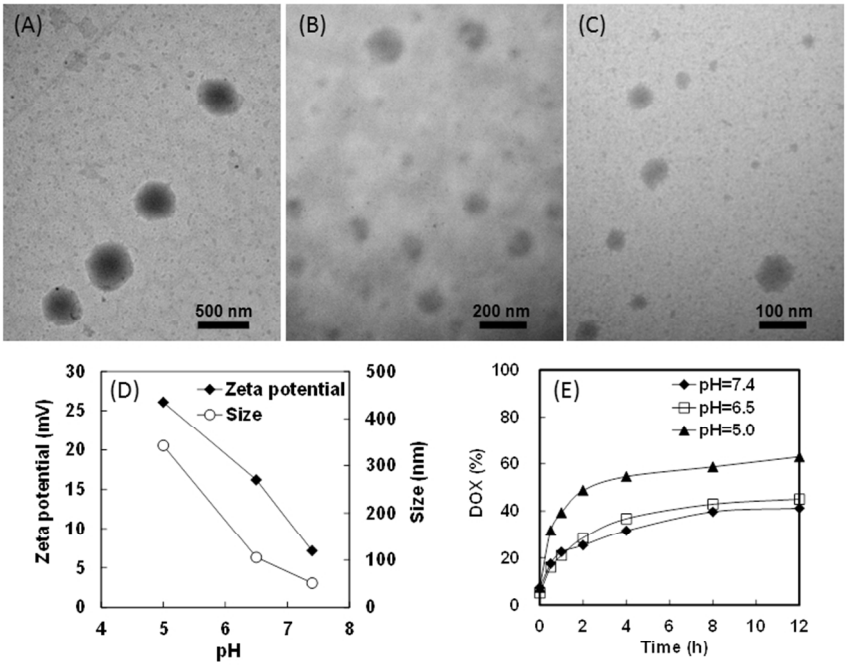

Figure 3. Properties of PDCZP nanocarriers. TEM images at pH 5.0 (A), pH 6.5 (B), and pH 7.4 (C). Size and zeta potential profiles at different pH (D). DOX release profiles of DOX-loaded PDCZP at different pH (E).
Figure 3
254x190mm (96 x 96 DPI)

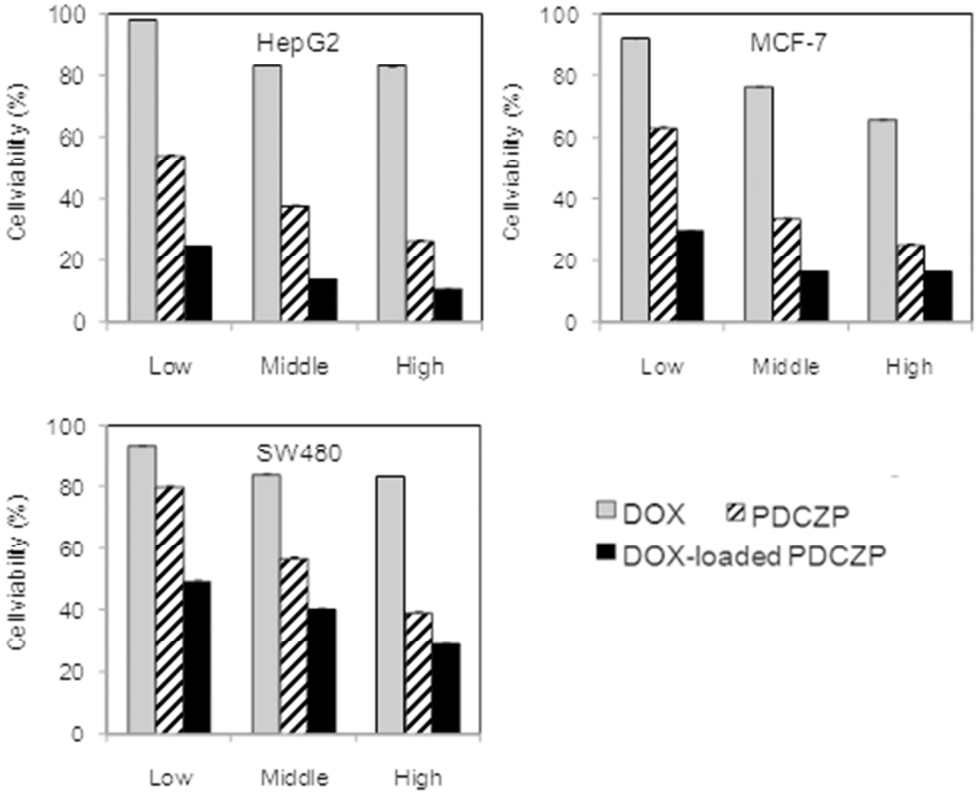

Figure 4. Cytotoxicity of DOX, PDCZP, and DOX-loaded PDCZP on the cancer cell lines, including HepG2, MCF-7, and SW480, respectively. "Low", "Middle", and "High" indicate the concentration levels of DOX (13.0, 31.1, 60.3 μM), PDCZP (40, 100, 200 μg/ml), and DOX-loaded PDCZP (DOX at 13.2, 31.8, 63.6 μM, and PDCZP at 50, 120, 240 μg/ml), respectively. All the data are presented as means ± SD (n=6).

Figure 4
42x36mm (300 x 300 DPI)

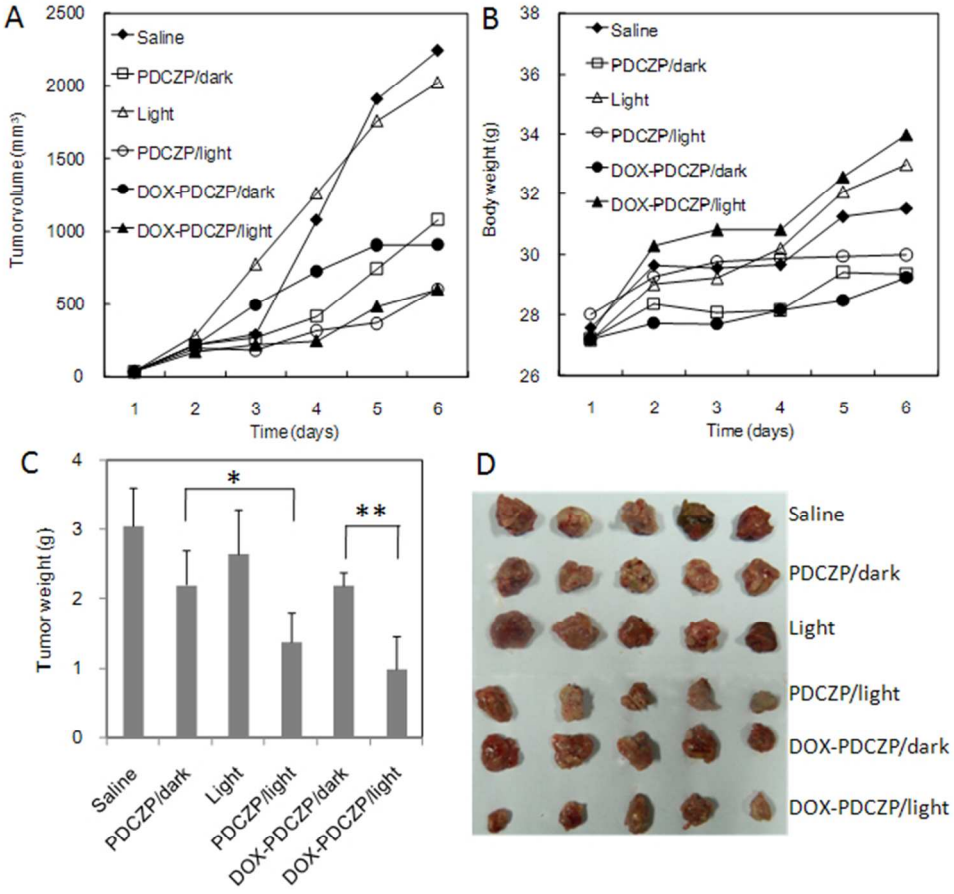

Figure 5. Anticancer effects of different medicines under dark conditions or lighting on the H22 tumor-bearing mice. Tumor volume profiles (A). Body weight profiles (B). Tumor weight after treatments (C). * $p < 0.05$; ** $p < 0.01$. (D) Tumors after treatments. All the data are presented as means ± SD (n=5).
Figure 5
58x56mm (300 x 300 DPI)

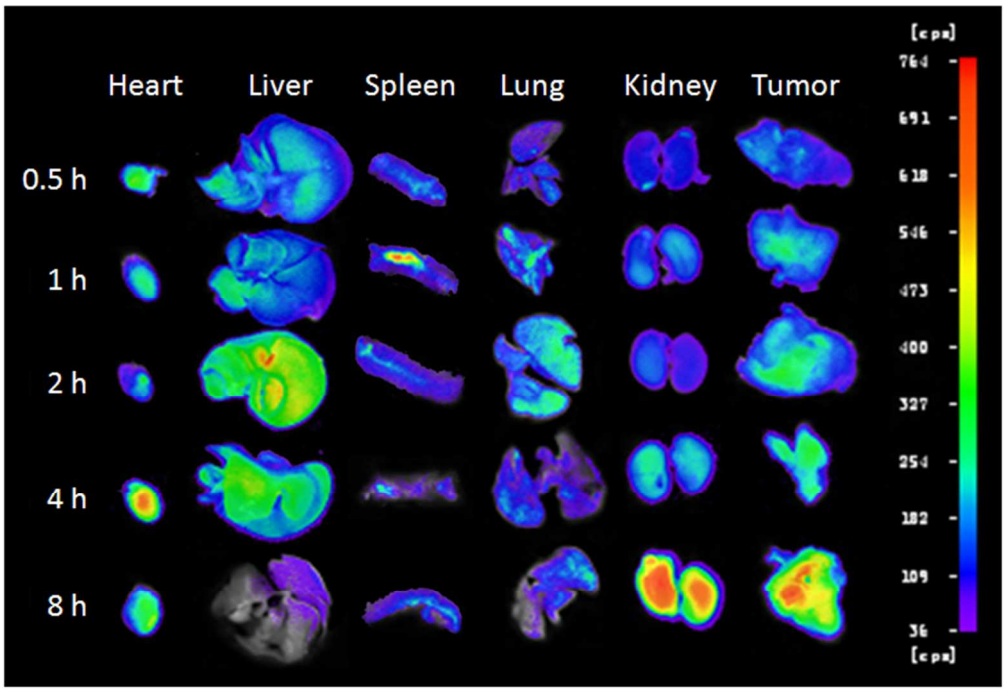

Figure 6. Fluorescence non-invasively tumor imaging after injecting the DOX-loaded PDCZP to the tumor-bearing mice.
Figure 6
61x42mm (300 x 300 DPI)

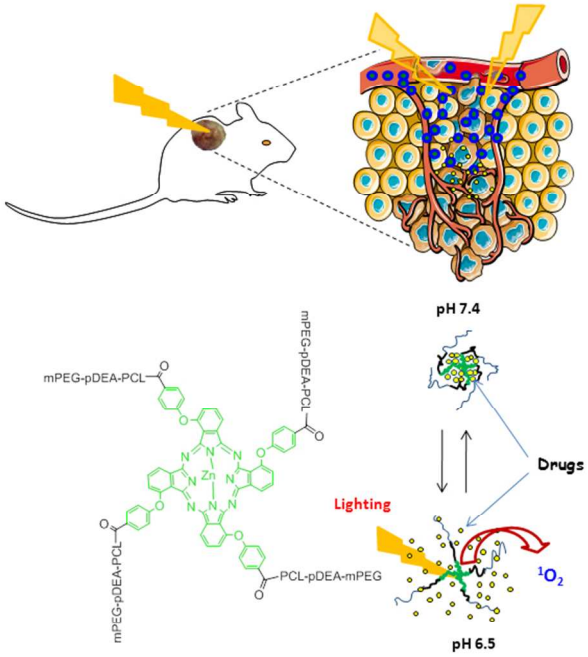

Table of Contents Graphic for manuscript
TOC Graphic
254x190mm (96 x 96 DPI)